3-D Finite Element Study of Embankment Resting on Soft Soil Reinforced with Encased Stone Column

B. K. Pandey, S. Rajesh, and S. Chandra

Abstract This paper presents the outcomes of a 3-D finite element analysis performed to study the time-dependent behavior of embankment resting on the geosynthetic-encased stone column (GESC). The numerical analysis is carried out on both fixed and floating GESC. The results of the study show the effect of encasement stiffness, encasement length and length of the geosynthetic encased stone column on time-dependent behavior of the system. The use of GESC has provided significant improvement in reducing the generation and dissipation of excess pore water pressure, settlement and lateral displacement of the column along its length. The study indicates that the higher stress concentration in the case of GESC results in better time-dependent behavior. Additionally, the results also confirm that there is an optimum value of encasement stiffness, encasement length and length of geosynthetic-encased column beyond which no substantial improvement is attained.

Keywords Soil improvement · Encased stone column · Geogrid

1 Introduction

The massive infrastructure projects require suitable ground conditions to supports its foundation. There are different ground improvement techniques available to mitigate the problems of the compressible soils. In the improvement of soft soil for projects like embankment fill supports, LNG/Oil storage tanks, railroad, and other miscellaneous structures, the use of stone columns has proven efficacious both regarding economy and performance. Moreover, it is very successful because of its advantages. It helps in slope stability improvement, increasing bearing capacity and time rate of settlement, reduction in total and differential settlement, reducing liquefaction potential Barksdale and Bachus ([1983](#)). The application of stone column serves it purpose if the undrained shear strength (C_u) of soil lies between 15 and 50 kPa. However, if the undrained shear strength of the soil is <15 kPa, then the confinement provided

B. K. Pandey (✉) · S. Rajesh · S. Chandra
Department of Civil Engineering, IIT Kanpur, Kanpur, Uttar Pradesh 208016, India
e-mail: balbir@iitk.ac.in

by the surrounding soil to the stone column is not adequate, and hence it fails in excessive settlement due to bulging. Therefore, reinforcing the stone column either by encasement or by placing the horizontal strip of geosynthetic within column body at regular interval provides the extra resistance against radial bulging of the column as reported by Alexiew et al. (2012) and Ali et al. (2012). In last two decades, various projects for the railroad and road embankment, bridge ramp, flood protection dike were accomplished using encased stone columns in Germany, Netherlands, Sweden and India (Raithel et al. 2005; Mahajan et al. 2016).

The idea of encasing the column in full or partially is studied experimentally by numerous researchers like (Raithel et al. 2004, 2005; Ayadat and Hanna 2005 ; Murugesan and Rajagopal 2006, 2007) under undrained condition. Furthermore, Najjar et al. (2010) studied the mode of failure and failure envelope of geosynthetic-encased stone columns (GESCs). Likewise, Dash and Bora (2013) reported the deformed shape of floating GESCs. Gu et al. (2016) quantified the effect of encasement length on stress concentration and radial strain. Miranda et al. (2017) explored the drained behavior of GESCs by considering the slice of the unit cell. Debnath and Dey (2017) reported increase in bearing capacity for geogrid-reinforced sand over GESC. In discovering the behavior of GESCs, the numerical modeling has also been extensively used. Yoo and Kim (2009) adopted unit cell (both 3D and axisymmetric) and full 3D model to compare the different modeling approach. Yoo (2010) by modeling quarter of column in 3D column model and full 3D model reported the effects of various parameters on GESCs behavior. Khabbazian et al. (2010) and Elsawy et al. (2010) observed that the encasement type and stiffness play an essential role in the response of the GESCs. Majority of the studies focus on unit cell approach (either 3D or axisymmetric or quarter column) by loading the column only or entire unit cell (Raithel et al. 2004; Elsawy et al. 2010; Castro and Sagaseta 2011; Fattah and Majeed 2012; Rajesh and Jain 2015; Rajesh 2017; Castro 2017 and others) or unit cell with embankment loading (Almeida et al. 2013; Elsawy 2013; Zhang and Zhao 2014; Hosseinpour et al. 2014, 2015). However, only limited study has been conducted in details considering the encasement parameter's (length and stiffness) and also GESC length on time-dependent responses under embankment loading. Therefore, there is a need for a comprehensive study to understand the modeling details as well as the behavior of GESC under the embankment loading.

This study focuses on understanding the effect of encasement length, encasement stiffness and length of GESC on the behavior of GESC under embankment loading through 3-D unit cell model. The impact of the parameters mentioned above is evaluated regarding settlement reduction, generation and dissipation of excess pore water pressure, lateral deformation of the column along its length and the stress concentration ratio.

2 Geometry and Model Description

Numerical analysis is performed using PLAXIS 3D, a finite element package (Brinkgreve et al. 2013). A hypothetical case study is formulated in the present study. The foundation soil consists of 9.5 m of soft clay underlying a 0.5 m of the sand platform. The sand platform serves as the drainage blanket and is laid before the embankment construction. The ground water table lies at the top of the clay surface, i.e., 0.5 m below the ground. The 3D unit cell is conceptualized from the central part of the embankment. The size of the unit cell model adopted is 2 m × 2 m × 10 m ($L \times B \times H$) with column installed at the center of the unit cell. The diameter (d) of GESC was worked out to be 0.8 m by considering spacing of GESC of 2 m arranged in a square pattern. Figure 1 shows the details of the GESC-reinforced soft ground considering 3D unit cell model. In the present study, the length of GESC (L_{GESC}) is varied between 5 and 10 m, and the axial stiffness of encasement is varied between 500 and 6000 kN/m (Murugesan and Rajagopal 2006; Khabbazian et al. 2010). The total height of the embankment is 6 m and is constructed in three stages; each stage is made of 2 m height, similar to the work carried out by Yoo (2010). The duration of each stage consists of two parts: one is construction period (t_{c1}, t_{c2}, and t_{c3}) and the other is rest period (t_{r1} and t_{r2}). The construction period is 20 days, and the rest period is 30 days. The rest period is provided for a partial dissipation of excess pore water pressure.

The displacement and hydraulic boundary conditions for the model are chosen based on the symmetry. Therefore, considering symmetry into account no displacement in the perpendicular direction of the symmetry plane and to the base is allowed (Yoo 2010). Congruently, at the symmetry plane, no flow at the boundary will take place. Therefore, the symmetry plane has been kept as a closed consolidation boundary. Moreover, the bottom boundary is also held closed consolidation boundary considering the impervious layer below the soft clay (Rajesh 2017). The soft soil is modeled using soft soil constitutive model material model. However, for the embankment, stone column and sand platform, a linear-elastic perfectly plastic model with Mohr–Coulomb failure criterion was used. Hardening soil can be used

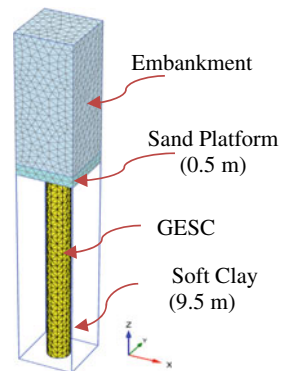**Fig. 1** Generated mesh connectivity plot and details for 3D unit cell

Table 1 Summary of the constitutive model and related parameter

Properties	Column (Mohr–Coulomb)	Soft clay (soft soil)	Platform (Mohr–Coulomb)	Embankment (Mohr–Coulomb)
	Chen et al. (2015)	Hosseinpour et al. (2014)	Huang et al. (2009)	Aljanabi et al. (2013)
γ (kN/m^3)	22	14.50	20	20
E (kPa)	40,000	750	20,000	20,000
ν	0.30	0.28	0.33	0.30
c' (kPa)	0.50	4	5	5
φ' (0°)	38	27.50	32	30
Ψ (0°)	10	–	–	–
C_c	–	1.26	–	–
C_s	–	0.097	–	–
k_h (m/day)	10.368	7.50×10^{-5}	1	1
k_v (m/day)	10.368	8.40×10^{-6}	1	1

Note E = tangential elastic modulus; ν = poisson's ratio; γ = soil unit weight; c' = cohesion of soil; φ' = soil friction angle; ψ = dilation angle; C_c = compressibility index; C_s = swelling index; k = permeability (subscript h and v corresponds to horizontal and vertical respectively); – = data not given

to represent the effect of strain rate on the behavior of granular materials. However, use of hardening soil model caused slow convergence problem while performing the parametric study. Hence, the modeling of stone column is limited to Mohr–Coulomb model. Table 1 summarizes the constitutive model and related parameters used in the analysis. The geogrid is used in the study and is modeled as an elastic material having orthotropic behavior. These are slender structures that can sustain only tensile force and no compression.

3   Mesh Sensitivity and Validation

The soft soil, sand platform and embankment were modeled using 10-node tetrahedral elements. The geogrid was modeled using 6-node triangular surface element. For modeling soil–geogrid interaction, joint elements (interfaces) were added to geogrid and surrounding soil. The interfaces comprised of 12-node interface elements with zero thickness. In the case of the material models like soft soil model and Mohr–Coulomb model, the primary interface parameter is the strength reduction factor (R_{inter}). The R_{inter} adopted in the present study for soft soil, sand platform, embankment and stone column are 1 as reported by Aljanabi et al. (2013), whereas for geogrid soil interface it is 0.7 as reported by Chen et al. (2015). The mesh generation process used in the study is fully automated. However, it also takes into account of soil profile and all the structural members as well as geometric and boundary conditions

Fig. 2 Mesh sensitivity analysis with a variety of elements for GESC
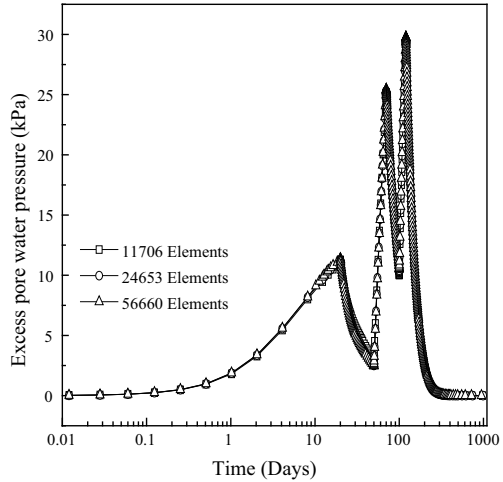
(Brinkgreve et al. 2013). From the previous studies, it has been observed that mesh should be adequately fine to get the precise results (Castro 2017). Figure 2 shows the generation and dissipation of excess pore pressure with time for the embankment resting on GESC. From Fig. 2, it can noticed that the fine mesh having 24,653 elements predicts 0.5–1.01% lower excess pore pressure as compared to very fine mesh with 56,660 elements. Moreover, the time taken for the analysis in the case of 56,660 elements is thrice as compared to 24,653 elements. Hence, for a lesser computational time without compromising with the accuracy, the fine mesh with numbers of element lying between 20 and 25 thousand has been chosen for further studies.

The present study is validated with the study conducted by Rajesh (2017) in which the surface load is applied on the top of an axisymmetric problem. However, in the present study, 3D unit cell having a square cross-sectional area of dimension 2.25 m × 2.25 m is used as reported by Rajesh (2017). All the material properties and the dimensions were kept intact, except properties of the plate. A steel plate of thickness (t_p) 30 mm, unit weight of steel (γ_{steel}) = 78.5 kN/m^3 and $E = 4.44 \times 10^6$ kN/m^2 is used for the loading. The linear isotropic constitutive model has been adopted for steel plate. The details of the constitutive model and related parameters for other materials can be found in the referred paper. Figure 3 shows the result of 3D unit cell compared with axisymmetric model of Rajesh (2017) for soft soil reinforced with ordinary stone column (OSC). The results show that model is in good agreement with the referred study.

Fig. 3 Validation with
Rajesh (2017) for OSC (very
fine mesh)
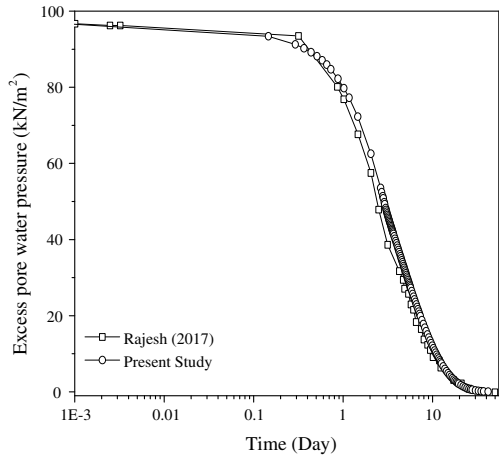
4 Results and Discussions

The primary emphasis of the study is to understand the effect of parameters like the effect of the encasement, length of the encasement, axial stiffness of the encasement and length of the geosynthetic encased stone column on time-dependent behavior of GESC. The length of the encasement (L_{ESC}) is normalized by the length of the ordinary stone column (L_{OSC}) and is expressed as, $\zeta = L_{ESC}/L_{OSC}$. Furthermore, the length of geosynthetic-encased stone column (L_{GESC}) is similarly normalized by the depth of the treatment ($H_{Treatment}$) which is expressed as $\xi = L_{GESC}/H_{Treatment}$. Finally, the results of the study have been discussed in detail for the different parameters in the ensuing sections below.

4.1 Effect of Encasement

The first parametric study emphasizes on the influence of using different column type, i.e., no column (directly on soft soil), ordinary stone column (OSC) and GESC beneath an embankment. The influencing effect is appraised regarding generation and dissipation of pore water pressure and settlement with time. The fully encased column having encasement stiffness of 2000 kN/m has been used in the case of GESC below the embankment. The monitoring point in the case of excess pore water pressure is at mid-depth in soft soil region. In Fig. 4, excess pore water pressure is plotted against time. This result displays that the excess pore water pressure generated at the end of construction period (120 days) varies for different cases. It is on the higher side, i.e., 117.112 kPa for the embankment on the soft soil, whereas 49.201 and 29.479 kPa for embankment on OSC and GESC, respectively. Further, it can be seen that the time taken to dissipate the excess pore water pressure to a level of 0.1 kPa for

Fig. 4 Excess pore pressure variation with time for soft soil, OSC and GESC
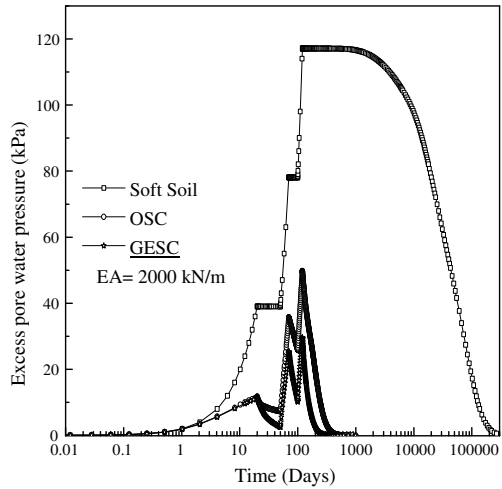
embankment resting on soft clay, OSC and GESC was 337, 255, 534 and 317 days, respectively. The lower value of pore pressure generation and faster dissipation in the case of GESC and OSC are attributed to different factors as reported by Han and Ye (2001). The factors influencing excess pore water pressure include reduction due to a decrease in vertical stress, increment due to increase in the lateral stress from the column and reduction due to drainage of water from the soil. Considering this, it is evident for embankment on GESC to perform better as compared to that on OSC because of additional stiffness provided by the encasement. Nevertheless, it is also perceived that the excess pore water pressure generation for the initial 2–3 days is insignificant because at this point the reinforced and unreinforced soil has negligible stress concentration ratio as they behave as an undrained condition.

In Fig. 5, settlement at the bottom of the embankment is plotted against the time (including construction and service time) for embankment resting on soft clay, OSC and GESC. The variation of settlement for different types of embankment support can be clearly understood. From the figure, it is observed that the settlement at the end of the consolidation period is 1.63, 1.13 and 0.44 m for embankment resting on soft clay, OSC and GESC, respectively, which foresees the settlement reduction factor (β) of 0.69 and 0.27 for OSC and GESC, respectively. The settlement reduction factor is the ratio of settlement at the surface after treatment (δ_{at}) w.r.t that of before treatment (δ_{bt}) and is expressed as $\beta = \delta_{at}/\delta_{bt}$. Furthermore, the difference in the settlement for soft soil, OSC and GESC in the initial 10 days is almost insignificant with maximum settlement of roughly 11 mm. Thus, it envisages the improved performance of GESC in reducing the settlement. The reason can be attributed to the lesser excess pore water pressure generation (as from Fig. 4) and increased stiffness due to encasement.

Fig. 5 Settlement variation with time at the surface for Soft clay, OSC and GESC
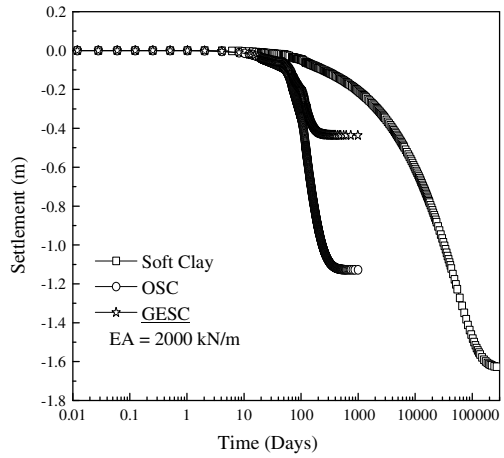
4.2 Effect of Encasement Stiffness

To study the influence of axial stiffness of different encasement stiffness varying between 500 and 6000 kN/m is adopted. In Fig. 6, excess pore water pressure generation and dissipation variation has been plotted with time for different stiffness of encasement. The figure displays that the excess pore water pressure generated at the end of the construction period varies between 20.26 and 41.55 kPa for different stiffness of encasement. The lower value of 20.26 kPa is observed for 6000 kN/m and 41.55 kPa for 500 kN/m stiffness. The variation of the generated excess pore water pressure is because lesser stresses are transferred to the soft clay because of the stiffer encasement. The difference is considerably lower (<5%) for stiffness of encasement lying between 4 and 5 thousand kN/m. Congruently, the time taken for

Fig. 6 Excess pore pressure variation with time for GESC having the different stiffness of encasement
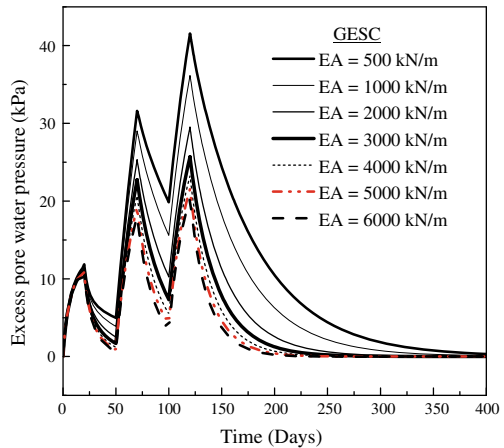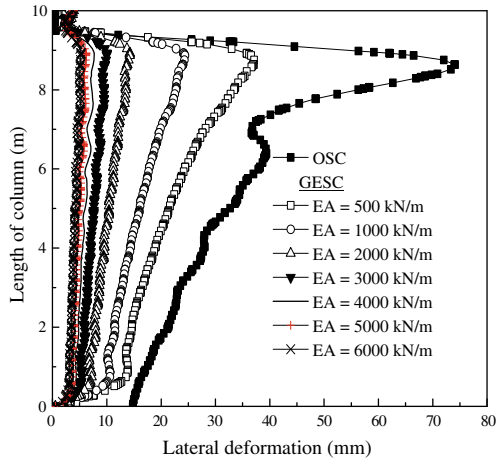
Fig. 7 Variation of lateral deformation of the column for OSC and GESC of different encasement stiffness


dissipating excess pore water pressure to 0.01 kPa is nearly 638 and 240 days, for stiffness 500 kN/m and 6000 kN/m, respectively. Moreover, the maximum difference in the time for stiffness lying between 4000 and 6000 kN/m is <16%. From this, we can say that the optimum stiffness of encasement can be 5000 kN/m for complete dissipation of excess pore water pressure. Using the encasement stiffness >5000 kN/m, there is no substantial enhancement in the performance is observed.

Figure 7 illustrates the lateral deformation of the OSC and GESC having the different stiffness of the encasement. As expected the lateral deformation in the case of OSC is 14.43 times higher as compared to GESC with stiffness of 6000 kN/m; however, it is 1.18 times for the encasement stiffness 5000 kN/m as compared to 6000 kN/m. From the previous studies (Barksdale and Bachus 1983; Christoulas et al. 2000; Murugesan and Rajagopal 2010; Malarvizhi and Ilamparuthi 2007; Yoo and Kim 2009), the maximum lateral deformation occurs at the depth varying between 2 and 3 * D from the top of the column. This maximum deformation depth is dependent on the loading area as well as the strength of the surrounding soil. In the current study as can be seen from Fig. 7, this depth is nearly 1.7 * D.

In Fig. 8, settlement reduction factor (β) is plotted against GESC improved ground having different encasement stiffness. However, from this figure we can clearly see that the difference in the settlement reduction by using GESC with encasement having stiffness 6000 kN/m is inconsequential (approx. 8%) as compared to encasement having 5000 kN/m stiffness. Therefore, we can evidently state that using encasement stiffness above 5000 kN/m has no significant effect on the settlement reduction.
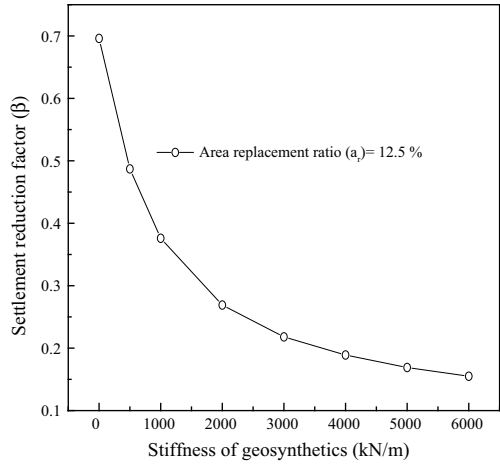
4.3 Effect of Encasement Length

The influence of encasement length on behavior of GESC is analyzed by varying
encasement length (ζ) from 0 to 1. The reference encasement stiffness used for this
parametric study is 2000 kN/m. In Fig. 9, the variation of excess pore water pressure
is plotted against time. The excess pore water pressure generation at the end of the
construction period, i.e., 120 days is maximum for encasement length (ζ) of 0.50,
whereas the difference in the generated excess pore water pressure is insignificant
after $\zeta = 0.75$. Moreover, the time taken to dissipate the generated excess pore
water pressure to a level of 0.1 kPa shows a slight variation of less than 2% for
encasement length (ζ) beyond 0.75. Additionally, the lateral bulging of the column
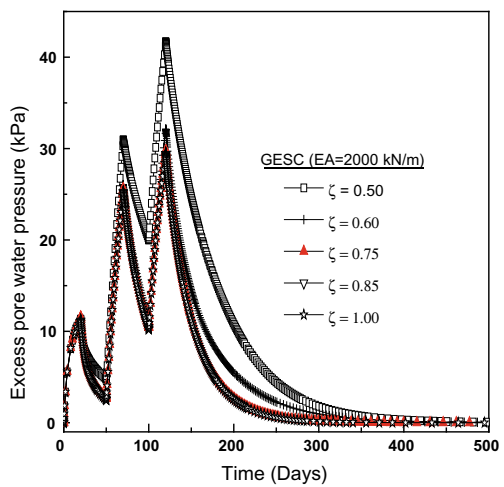
is dominant at the location where encasement terminates at the bottom as can be noticed from Fig. 10. In this figure, lateral deformation against depth from the top of the column for GESC having different encasement length is plotted. However, this lateral deformation in the case of the encased column is almost twice as compared to column without encasement (i.e., OSC) at the point of termination of the encasement (example let's say at 5 m from the top for $\zeta = 0.50$).

Similarly, in Fig. 11, settlement reduction factor (β) is plotted against embankment resting on GESC improved ground having varying encasement length. From this figure, it can be observed that full encasement of the column results in significant reduction in the settlement (>61%) as compared to the column without encasement. Moreover, the variance in the settlement reduction (β) for $\zeta = 0.75$ and $\zeta = 0.85$ w.r.t, $\zeta = 1$ is approximately 21% and 16%, respectively. Seeing this variation, one

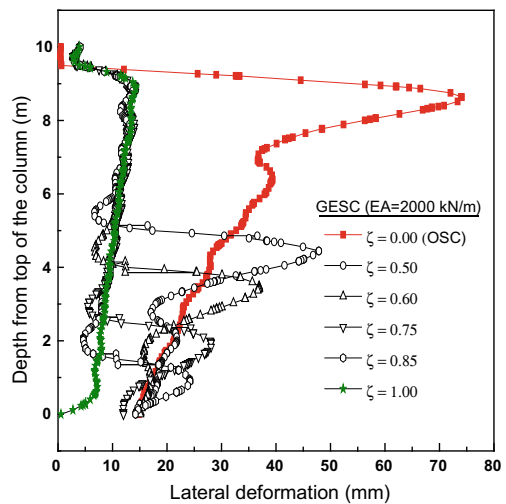**Fig. 10** Lateral deformation of GESC having different encasement length

Fig. 11 Settlement reduction factor for GESC having varying encasement length
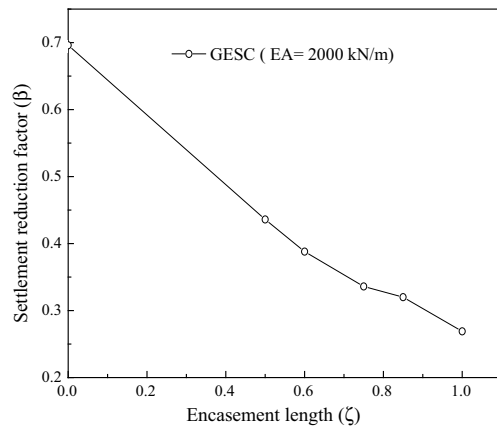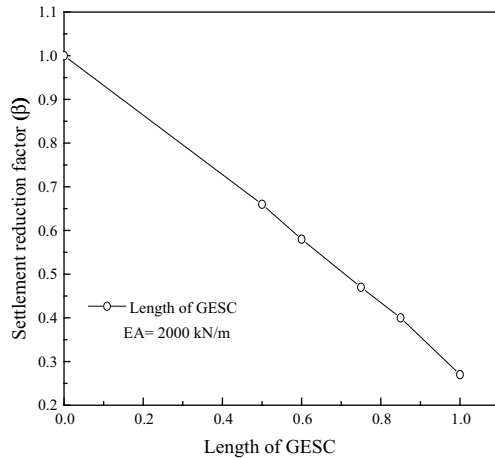
Fig. 12 Settlement reduction factor for embankment resting on GESC having varying length of GESC


can state that the fully encased stone column contributes significant reduction in the settlement when compared to partially encased GESC.

4.4 Effect of Length of GESC

As already mentioned, the above discussions were based on the influence of properties of encasement considering fixed end column. However, the behavior of embankment resting on the floating GESC is reported in this segment. In Fig. 12, settlement reduction factor (β) is plotted against GESC improved ground having varying length of GESC.

The encasement stiffness was kept fixed at 2000 kN/m. From the figure, it is noticeable that the settlement reduction in the case of GESC length (ξ) of 1.00 is approximately 73% as compared to without improvement. Furthermore, the difference in the reduction is roughly 15% for GESC length (ξ) of 0.85 as compared to GESC length (ξ) of 0.75. This reduction in settlement values indicates that using GESC length (ξ) of 1.00, i.e., the end bearing GESC is more useful as compared to floating GESC. Similarly, the generated excess pore water pressure at the end of the construction period (120 days) is nearly 58% lower for GESC length (ξ) of 1.00 as compared to 0.5. Correspondingly, the time taken to dissipate the generated excess pore water pressure to a level of 0.1 kPa is also reduced by almost 94% as can be perceived from Fig. 13. From this discussion, we can infer that the performance of the end bearing GESC, i.e. having GESC length (ξ) of 1.00, is relatively high as compared to floating GESC.

Fig. 13 Excess pore pressure variation with time for GESC having different length of GESC
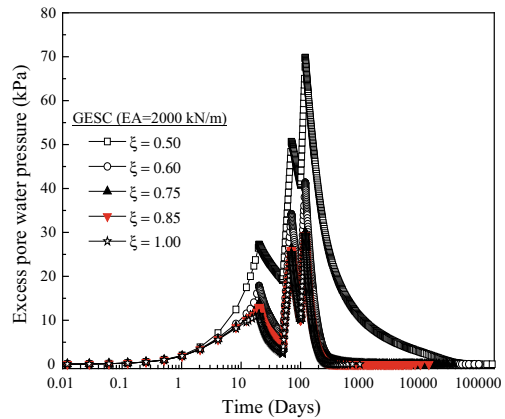
5 Conclusion

The paper presents an organized numerical analysis of embankment resting on a geosynthetic encased stone column. The area replacement ratio in this study is kept constant at 12.5%. From the study, following points are concluded.

- Encasing the stone column significantly helps in (75%) reduction in generation of excess pore water pressure and at the same time (73%) reduction in the settlement as compared to embankment resting on soft soil, for the case analyzed in this study.
- The stiffness of the encasement plays a critical effect on the time-dependent behavior of the embankment resting on the GESC. However, the use of encasement stiffness greater than 5000 kN/m doesn't show significant improvement.
- The fully encased stone column shows substantial improvement regarding the time-dependent behavior of embankment resting on GESC as compared to partial encasement of GESC.
- The performance of fixed end GESC column outweighs the floating GESC supporting an embankment.

The presented study is primarily based on finite element simulations; further experimental investigations are required to confirm the outcomes.

References

Alexiew D, Raithel M, Kuster V, Detert O (2012) 15 Years of experience with geotextile encased granular columns as foundation system. In: ISSMGE - TC 211 international symposium on ground improvement IS-GI, Brussels

Ali K, Shahu JT, Sharma KG (2012) Model tests on geosynthetic-reinforced stone columns: a comparative study. Geosynth Int 19(4):292–305

Aljanabi QA, Chik Z, Kasa A (2013) Construction of a new highway embankment on the soft clay soil treatment by stone columns in Malaysia. J Eng Sci Technol 8:448–456

Almeida MSS, Riccio M, Hosseinpour I (2013) Performance of a geosynthetic-encased column (GEC) in soft ground: numerical and analytical studies. Geosynth Int 20:252–262

Ayadat T, Hanna AM (2005) Encapsulated stone columns as a soil improvement technique for collapsible soil. Proc Inst Civ Eng Ground Improv 9:137–147

Barksdale RD, Bachus RC (1983) Design and construction of stone column, vol 1. U.S Department of Transportation, Report No—FHA FHWA/RD-83 (1983)

Brinkgreve RBJ, Engin E, Swolf WM (2013) Plaxis 3D 2013 manual. Plaxis Bv, The Netherlands

Castro J (2017) Groups of encased stone columns: influence of column length and arrangement. Geotext Geomembr 45:68–80

Castro J, Sagaseta C (2011) Deformation and consolidation around encased stone columns. Geotext Geomembr 29:268–276

Chen J-F, Li L-Y, Xue J-F, Feng S-Z (2015) Failure mechanism of geosynthetic-encased stone columns in soft soils under embankment. Geotext Geomembr 43:424–431

Christoulas S, Bouckovalas G, Giannaros C (2000) An experimental study on model stone columns. Soil Found 40(6):11–22

Dash SK, Bora MC (2013) Improved performance of soft clay foundations using stone columns and geocell-sand mattress. Geotext Geomembr 41:26–35

Debnath P, Dey AK (2017) Bearing capacity of geogrid reinforced sand over encased stone column in soft clay. Geotext Geomembr 45(6):653–664

Elsawy MBD (2013) Behavior of soft ground improved by conventional and geogrid-encased stone columns, based on FEM study. Geosynth Int 20:276–285

Elsawy M, Lesny K, Richwien W (2010) Performance of geogrid-encased stone columns as a reinforcement of soft ground. In: Benz T, Nordal S (eds) Numerical methods in geotechnical engineering. Taylor and Francis Group, London UK, pp 875–880

Fattah MY, Majeed QG (2012) Finite element analysis of geogrid encased stone columns. Geotech Geol Eng J 30:713–726

Gu M, Zhao M, Zhang L, Han J (2016) Effects of geogrid encasement on lateral and vertical deformations of stone columns in model tests. Geosynth Int 23:100–112

Han J, Ye S-L (2001) Simplified method for consolidation rate of stone column reinforced foundations. J Geotech Geoenviron Eng 127(7):240–248

Hosseinpour I, Riccio M, Almeida MSS (2014) Numerical evaluation of a granular column reinforced by geosynthetics using encasement and laminated disks. Geotext Geomembr 42:363–373

Hosseinpour I, Almeida MSS, Riccio M (2015) Full-scale load test and finite-element analysis of soft ground improved by geotextile-encased granular columns. Geosynth Int 22:428–438

Huang J, Han J, Oztoprak S (2009) Coupled mechanical and hydraulic modeling of geosynthetic-reinforced column-supported embankments. J Geotech Geoenviron Eng 135(8):1011–1021

Khabbazian M, Kaliakin VN, Meehan CL (2010) Numerical study of the effect of geosynthetic encasement on the behaviour of granular columns. Geosynth Int 17:132–143

Mahajan R, Korulla M, Rimoldi P (2016) Geotextile encased columns design and installation. In: Proceedings of the 6th Asian regional conference on geosynthetics-geosynthetics for infrastructure development, New Delhi, India, pp 188–194

Malarvizhi SN, Ilamparuthi K (2007) Comparative study on the behavior of encased stone column and conventional stone column. Soils Found 47(5):873–885

Miranda M, Costa DA, Castro J, Sagaseta C (2017) Influence of geotextile encasement on the behaviour of stone columns: laboratory study. Geotext Geomembr 45:14–22

Murugesan S, Rajagopal K (2006) Geosynthetic-encased stone columns: numerical evaluation. Geotext Geomembr 24:349–358

Murugesan S, Rajagopal K (2007) Model tests on geosynthetic-encased stone columns. Geosynth Int 14(6):346–354

Murugesan S, Rajagopal K (2010) Studies on the behavior of single and group of geosynthetic encased stone columns. J Geotech Geoenviron Eng 136(1):129–139

Najjar SS, Sadek S, Maakaroun T (2010) Effect of sand columns on the undrained load response of soft clays. J Geotech Geoenviron Eng 136:1263–1277

Raithel M, Küster V, Lindmark A (2004) Geotextile-encased columns—a foundation system for earth structures, illustrated by a Dyke project for works extension in Hamburg. In: Proceedings of the Nordic geotechnical meeting NGM, Ystad, Sweden, pp 1–10

Raithel M, Kirchner A, Schade C, Leusink E (2005) Foundation of construction on very soft soil with geotextile encased column—state of the art. In: Proceedings of geo-frontiers 2005, Austin, Texas, United States, pp 1–11

Rajesh S (2017) Time-dependent behaviour of fully and partially penetrated geosynthetic encased stone columns. Geosynth Int 24:60–71

Rajesh S, Jain P (2015) Influence of permeability of soft clay on the efficiency of stone columns and geosynthetic encased stone columns—a numerical study. Int J Geotech Eng 9(5):483–493

Yoo C (2010) Performance of geosynthetic-encased stone columns in embankment construction: numerical investigation. J Geotech Geoenviron Eng 136:1148–1160

Yoo C, Kim S-B (2009) Numerical modeling of geosynthetic-encased stone column-reinforced ground. Geosynth Int 16:116–126

Zhang L, Zhao M (2014) Deformation analysis of geotextile-encased stone columns. Int J Geomech 15:1–10